VIP Zeolite Catalysis Very Important Paper

DOI: 10.1002/ange.201303498

A Common Intermediate for N_2 Formation in Enzymes and Zeolites: Side-On Cu–Nitrosyl Complexes**

Ja Hun Kwak, Jong H. Lee, Sarah D. Burton, Andrew S. Lipton, Charles H. F. Peden, and János Szanyi**

Understanding the mechanisms of catalytic processes requires the identification of reaction centers and key intermediates, both of which are often achieved by the use of spectroscopic characterization tools. Owing to the heterogeneity of active centers in heterogeneous catalysts, it is frequently difficult to identify the specific sites that are responsible for the overall activity. Furthermore, the simultaneous presence of a large number of surface species on the catalyst surface often poses a great challenge for the unambiguous determination of the relevant species in the reaction mechanism. In contrast, enzymes possess catalytically active centers with precisely defined coordination environments that are only able to accommodate intermediates relevant to the specific catalytic process. Here we show that side-on Cu^+–NO^+ complexes, characterized by both high magnetic field solid state (SS) magic angle spinning (MAS) nuclear magnetic resonance (NMR) and Fourier transform infrared (FTIR) spectroscopy, are the key intermediates in the selective catalytic reduction of NO over Cu-SSZ-13 zeolite catalysts. Analogous intermediates have been observed and characterized in nitrite reductase enzymes, and shown to be the critical intermediates in the formation of N_2 for anaerobic ammonium oxidation reactions.[1] The identification of this key reaction intermediate, combined with the results of our prior kinetic studies, allows us to propose a new reaction mechanism for the selective catalytic reduction of NO with NH_3 under oxygen-rich environments over Cu-SSZ-13 zeolites, a key reaction in automotive emission control.

Denitrification and anaerobic ammonium oxidation are two processes that account for the release of fixed nitrogen as molecular nitrogen (N_2) into our atmosphere. A recent study by Kartal, et al. has shown that hydrazine (N_2H_4), a key intermediate in the path to N_2 in biological systems, is produced by anaerobic ammonium oxidation, and that NO was a direct precursor to the formation of N_2H_4.[1] This study also clearly establishes a crucial role for a side-on copper-nitrosyl species in the enzymatic production cycle of N_2. Two types of nitrite reductase enzymes, which contain Cu or Fe porphyrin cofactors as active centers, exist. The Fe-containing enzyme forms N-coordinated Fe–NO_2^- and Fe–NO intermediates during the catalytic cycle.[2,3] In the nitrite reductase with copper active centers, the binding of NO was controversial until the work of Tocheva, et al. determined an unprecedented side-on Cu nitrosyl configuration, which provided new insights into the catalytic mechanism of this enzyme.[4] A crystallography study on amine oxidase demonstrated the formation of a copper nitrosyl complex in which the Cu-N–O bond angle was determined to be 117°, a value approaching a side-on configuration. Side-on binding of diatomic molecules (NO and O_2) to Fe centers of enzyme catalysts are much better known. For example, in nitroporphirin 4, a ferric heme–NO complex was observed with Fe–N and Fe–O bond distances of 2.0 Å and 2.6 Å, respectively.[5] In naphthalene dioxygenase, side-on O_2 binding was observed, with Fe–O bond distances of 2.2 Å and 2.3 Å.[6] Side-on NO binding to Fe has also been reported in non-biological systems; for example, nitroprusside with Fe–N and Fe–O bond distances of 1.89 Å and 2.07 Å, respectively.[7] In a striking similarity to nitrite reductase enzymes, the most efficient heterogeneous catalysts for the selective catalytic reduction (SCR) of NO also contain either Cu or Fe ions as active centers located in ion-exchange positions in metal-ion-exchanged zeolites.[8] Thus, the two key common features of the enzymatic and heterogeneous catalytic systems are the identical nature of their catalytic active centers (the metal ions Cu and Fe), and the very well-defined coordination environment around these active sites (functional groups around the active center in enzymes and the zeolite framework itself).

Metal-ion-exchanged zeolites have been extensively studied for over thirty years for the SCR of NO_x, either with NH_3 or with hydrocarbons in the presence of excess oxygen.[8] Although, these materials show high efficiency for NO_x reduction, their practical applications were hindered by the

[*] J. H. Kwak
School of Nano-Bioscience & Chemical Engineering, Ulsan National Institute of Science and Technology (UNIST)
Ulsan 689-798 (Korea)
E-mail: jhkwak@unist.ac.kr

J. H. Lee,[+] C. H. F. Peden, J. Szanyi
Institute for Integrated Catalysis, Pacific Northwest National Laboratory, Richland, WA 99354 (USA)
E-mail: janos.szanyi@pnnl.gov

S. D. Burton, A. S. Lipton
Environmental Molecular Sciences Laboratory, Pacific Northwest National Laboratory, Richland, WA 99354 (USA)

[+] Current address: Daimler Trucks North America
Detroit, MI (USA)

[**] The authors acknowledge the US Department of Energy (DOE), Office of Energy Efficiency and Renewable Energy/Vehicle Technologies Program for support of this work. The research described in this paper was performed at the Environmental Molecular Sciences Laboratory (EMSL), a national scientific user facility sponsored by the DOE's Office of Biological and Environmental Research and located at Pacific Northwest National Laboratory (PNNL). PNNL is operated for the US DOE by Battelle Memorial Institute.

Supporting information for this article is available on the WWW under http://dx.doi.org/10.1002/anie.201303498.

inherent hydrothermal instabilities of the zeolite structures themselves.[9] The remarkable hydrothermal stability of a recently synthesized small-pore zeolite with a chabasite structure (SSZ-13), however, spurred renewed interest in commercializing zeolite-based NH_3 SCR catalysts.[10–12] In comparison to other previously studied zeolite-based SCR catalysts (such as, Cu-ion-exchanged ZSM-5, Y, FAU, and beta), Cu-SSZ-13 exhibits very high N_2 selectivity (low N_2O yield) and very low NO oxidation activity.[11,13] This latter observation is very important in light of the generally accepted NO reduction mechanism over zeolite-based SCR catalysts, which assumes that the initial step in the overall process is the oxidation of NO into NO_2 in the presence of a large excess of O_2.[8] Indeed, for some metal-exchanged zeolites the NO_x reduction rate was much higher when a reactant gas mixture containing NO and NO_2 in a 1:1 ratio was used (so-called "fast" SCR reaction), than with either NO or NO_2 alone.[14] In contrast, the addition of NO_2 did not significantly increase the reaction rate over Cu-SSZ-13.[15] These observations seem to suggest that the mechanism by which NO is reduced over this CHA-based catalyst might be fundamentally different from that observed for other zeolites. To unravel the mechanism of SCR over this catalyst, we investigated the surface species present upon exposure of Cu-SSZ-13 to NO using both ^{15}N solid state MAS-NMR and FTIR spectroscopy.

The formation of a Cu^+–NO^+ complex upon exposure of Cu-ion-exchanged SSZ-13 zeolites to NO was confirmed by FTIR studies.[16] The FTIR spectra (for detailed experimental conditions, see the Supporting Information) displayed in Figure 1 show absorption features characteristic of the

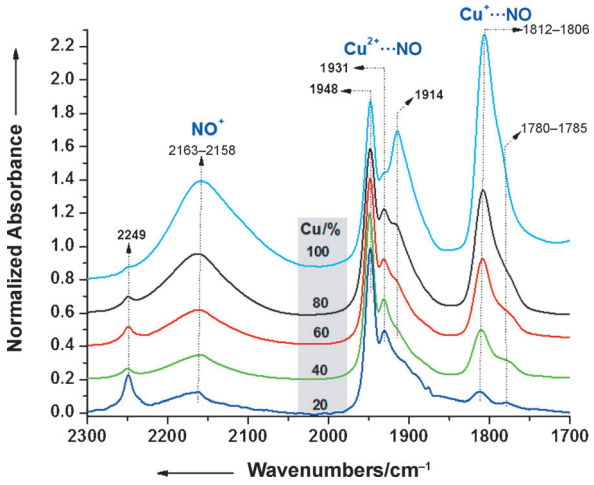

Figure 1. FTIR spectra obtained from pre-oxidized Cu-SSZ-13 zeolites with varying Cu-ion-exchange levels after their exposure to saturating amounts of NO at room temperature.

stretching vibrations of adsorbed NO species: NO adsorbed onto either Cu^+ (1812–1806 cm^{-1}), or Cu^{2+} (1900–1950 cm^{-1}), and an NO^+ species coordinated to Cu^+. The formation of NO^+ on Cu^{2+}-SSZ-13 can occur in two different ways: either by the disproportionation of NO_2,

$$2\,NO_2 \rightleftharpoons NO^+ + NO^{3-} \quad (1)$$

or by a redox reaction between Cu^{2+} and NO.

$$Cu^{2+} + NO \rightleftharpoons Cu^+NO^+ \quad (2)$$

As the FTIR experiments (Figure 1) were conducted in the absence of NO_2, the first NO^+ formation path can be ruled out. Instead, the amphoteric NO molecule, which possesses an unpaired electron, can reduce a Cu^{2+} ion and form the $Cu^+\cdots NO^+$ adduct, thus preserving charge balance in the zeolite framework. The resulting Cu^+ ions, in turn, can now interact with unreacted NO molecules to form Cu^+–nitrosyls, which is evidenced by the development of an IR band centered at 1810 cm^{-1}. Indeed, the FTIR spectra in Figure 1 show a clear correlation between the intensities of the IR features representing NO^+ (ca. 2160 cm^{-1}), and Cu^+–nitrosyls (ca. 1812 cm^{-1}). It is also evident from the FTIR data shown that the formation of NO^+ is correlated with the Cu content of the SSZ-13 structure; notably, the higher the Cu-ion-exchange level, the higher the amount of NO^+ formed. Interestingly, the Cu^{2+} ions, which are present at low Cu loading and known to be located in the windows of the double six-membered prisms of the chabasite structure,[12,17] bind NO relatively weakly and do not seem to participate in the formation of NO^+. This may be a consequence of the high coordination of these Cu^{2+} ions to oxygens in the zeolite framework, which renders them less reactive toward NO. With increasing ion-exchange levels, the number of a second type of Cu^{2+} ions, which are located in the large cavities of the chabasite structure and close to the eight member ring openings, increase, as do the number of NO^+ and Cu^+-nitrosyl species.[17] These Cu^{2+} ions are readily accessible to NO molecules, and seem to bind them quite strongly. Under catalytic conditions, however, Cu^{2+} ions located in the windows of the six-membered rings become accessible to NO, as they strongly interact with water and NH_3 molecules.[16] The chemical properties of these two types of Cu^{2+} ions (for example, reducibility) under these conditions are very similar.[18]

The necessity of the presence of Cu^{2+} ions in specific cationic positions to form NO^+ was also confirmed by the results of an FTIR experiment in which a Cu-SSZ-13 sample was reduced with CO at 573 K prior to NO exposure. The FTIR spectrum recorded from the CO-reduced Cu-SSZ-13 sample after NO exposure reveals the presence of NO adsorbed onto both unreduced Cu^{2+} (located primarily in the six-membered rings) and Cu^+ sites (Figure S1). The IR feature with the highest intensity is the one representing Cu^+–NO (ca. 1808 cm^{-1}), followed by the one originating from Cu^{2+}-adsorbed NO (ca. 1948 cm^{-1}). In contrast, the intensity of the IR band for the NO^+ species is very low, as most of the Cu^{2+} sites in the large cavities of the chabasite framework have been reduced to Cu^+ prior to NO adsorption. We have also established that an NO^+ species can be formed on these zeolites by the disproportionation of NO_2. Notably, when a pre-oxidized sample was exposed to NO_2, IR features with high intensity developed in both the 1250–1650 cm^{-1} and 2100–2300 cm^{-1} regions; these represent vibrations of ad-

sorbed nitrates and NO^+/NO^+NO_2 species, respectively (Figure S2). However, in the case where a $Cu^+\cdots NO^+$ species was formed by the reaction between Cu^{2+} and NO, no IR features representing nitrates (in the 1250–1650 cm^{-1} region) were observed. Thus, although Equation 1 is possible when Cu-SSZ-13 is exposed to NO_2, the lack of nitrates following NO adsorption demonstrates that Equation 2 is responsible for NO^+ formation in this latter case.

The interaction of NO with Cu-SSZ-13 was also investigated by ^{15}N solid state MAS-NMR spectroscopy, with the specific aim to obtain information about the nature and the structure (more specifically, the bonding geometry) of the Cu^+–NO^+ adduct we observed by FTIR spectroscopy. Figure 2 shows a series of ^{15}N SS-MAS-NMR spectra

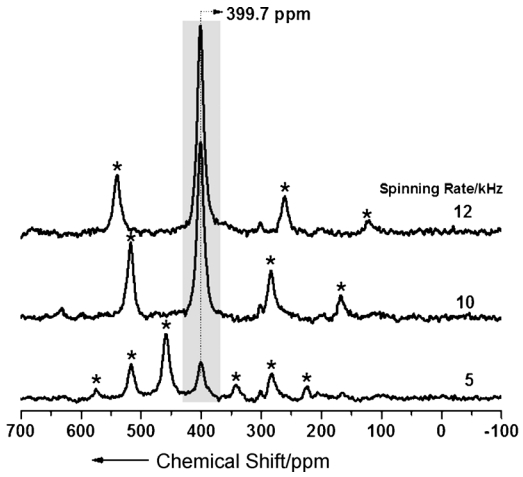

Figure 2. ^{15}N SS-MAS-NMR spectra of room-temperature ^{15}NO-exposed Cu-SSZ-13 at different spinning rates. Asterisks indicate spinning side bands.

recorded from a Cu-SSZ-13 sample after its exposure to ^{15}NO at room temperature using spinning rates of 5, 10, and 12 kHz. In each spectrum, equally spaced spinning side bands appear on both sides of the isotropic chemical shift centered at $\delta = 399.7$ ppm and assigned to a NO^+ species. We need to emphasize here that, owing to paramagnetic line broadening, neither molecularly adsorbed NO nor Cu^{2+}-bonded NO_x species are expected to be observed in the ^{15}N NMR spectra. Therefore, the only reasonable assignment of the isotropic NMR peak is the Cu^+-bound NO^+. Even more interesting is the information we can extract from the spinning side bands: they clearly suggest a three-dimensional anisotropic environment for the nitrogen atom in the adsorbed NO^+ species. In particular, the data presented in Figure 2 clearly indicate that the motion of the NO^+ species is frozen in a certain conformation. The coordination environment (the structure of the zeolite framework) of the copper ion is a key factor responsible for the restricted motion of the NO^+ ion. In general, it is very difficult to obtain detailed structural information of adsorbed NO species in Cu zeolites by NMR spectroscopy; primarily owing to the fact that fast motion of the adsorbate wipes out structural information. Thus, it is especially interesting that, in small pore zeolites (such as SSZ-13), adsorbed NO in the Cu^+–NO^+ complex can freeze into a conformation determined by both the location of the Cu^{2+} ions and their coordination environment (zeolite framework).

Fitting the sideband pattern, we determined the anisotropic shielding tensor, where the magnitude of the shielding anisotropy is $\delta = -230.2$ ppm, with an asymmetry parameter of 0.15. The agreement between the experimental and simulated NMR spectra (shown in Figure S3 for 5 kHz spinning rate) is excellent. The principal components of the shielding tensor were determined; the anisotropy is defined as $\Delta = \delta_{33} - \delta_{iso}$, where the elements of the shielding tensor are ordered as $|\delta_{33}\text{-}\delta_{iso}| \geq |\delta_{11}\text{-}\delta_{iso}| \geq |\delta_{22}\text{-}\delta_{iso}|$. The asymmetry parameter (η) is defined as $(\delta_{22}\text{-}\delta_{11})/(\delta_{33}\text{-}\delta_{iso})$, and a value of zero indicates axial symmetry (at least a three-fold rotation). As the observed η is non-zero, we infer that there is no axial symmetry here, and thus the Cu-N-O atoms are not co-linear.

To interpret the NMR results more completely, a model of the Cu-SSZ-13 was constructed starting from the structure reported by Fickel and Lobo.[19] The model is expanded to several unit cells, initially with all silicon atoms, and then aluminum atoms are substituted, such that the SiO_2/Al_2O_3 ratio is 12:1. The aluminum atoms are placed such that no two are adjacent and at least one is near the known[12,19] copper site in the face of the six-membered rings of the zeolite. The second Cu^+ is placed in the center of an eight-membered ring with a NO attached to it. The cluster is then trimmed down to a minimal set of atoms and terminated with hydroxyls. Utilizing a DFT calculation (NWChem)[20] with the Becke three-parameter Lee–Yang–Parr (B3LYP) functional[21] and an Ahlrichs double-ζ basis set with polarization (pAVDZ)[22] the positions of the protons, Cu^+ ions and the NO are then optimized with fixed positions for the Si/Al and oxygen atoms. The optimized geometry, shown in Figure 3, provides a Cu-N-O angle (α) of 146.7°, which is somewhat larger than expected for a perfect side-on adsorption complex. The longer Cu–O than Cu–N bond distance, however, may originate from the interaction of the adsorbed NO^+ species with the surrounding ions of the zeolite framework. The structure of the Cu^+-NO^+ adduct, as determined by analysis of the NMR data, is very similar to the side-on copper–nitrosyl complex observed in Cu–nitrite reductase enzymes in biological systems.[4]

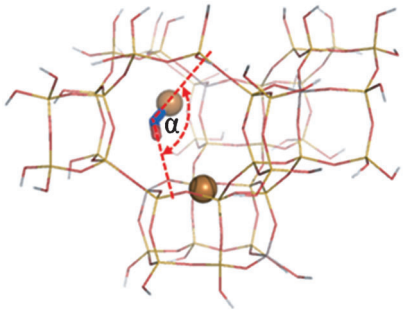

Figure 3. DFT optimized geometry of a Cu–NO adduct in Cu-SSZ-13. ($\alpha = 146.7°$)

The important question about these experimental results is the relevance of the above-discussed $Cu^+\cdots NO^+$ species to

the mechanism of the SCR of NO with NH_3 on Cu-SSZ-13 zeolites. To understand the mechanistic importance of this species, we need to recall some of the key findings of prior kinetic measurements on this system: very high N_2 selectivity, low NO oxidation activity, and the essential role of water in achieving high SCR activity.[11,13] The findings of McEwen, et al., showing that Cu^+ species are present under standard SCR conditions, as reported in their in operando EXAFS study, are also very important.[23] Notably, this work clearly establishes the presence of both Cu^+ and Cu^{2+} ions during the SCR of NO with NH_3 over the Cu-SSZ-13 catalyst. In prior mechanistic studies on other Cu- (and Fe) ion-exchanged zeolites (in particular, on Cu(Fe)-ZSM-5 or Beta) the primary role of the Cu (Fe) centers was assumed to be the oxidation of NO into NO_2. The resulting NO_2 could then disproportionate to form a $NO^+NO_3^-$ species which, in turn, was shown to be responsible for the formation of NH_4NO_2 and NH_4NO_3. Owing to the limited thermal stabilities of these two compounds, they were proposed to decompose into $N_2 + H_2O$, and $N_2O + H_2O$, respectively. NH_4NO_3 was also reported to further react with NO to form NH_4NO_2 and NO_2.[8,14] This mechanism could well explain the formation of significant amounts of N_2O over the metal-exchanged ZSM-5 and Beta catalysts, as well as the need for the presence of NO_2 to achieve high reactivity in "Fast" SCR.

Although the change in the oxidation state of the metal cation in ion-exchange positions within the zeolite has been claimed to be mechanistically important, the reactions in which this redox process would take place have not been elaborated on clearly. In biological systems, in contrast, the variation of the oxidation state of Cu has been clearly established in both the denitrification and anaerobic ammonium oxidation processes. Furthermore, the crucial role of the side-on copper–nitrosyl in nitrite reductase enzyme (discussed above) in the mechanism of molecular-nitrogen formation has been clarified. Here, we propose that the side-on $Cu^+\cdots NO^+$ species we have spectroscopically identified is an important intermediate in the SCR of NO with NH_3 over the Cu-SSZ-13 catalyst.

Combining the spectroscopic evidence of this study with the results of prior kinetic measurements, we now propose a reaction mechanism that is fully consistent with these observations (Figure 4). The first step of the proposed reaction mechanism is the reduction of Cu^{2+} to Cu^+ by NO, and the formation of the side-on $Cu^+\ldots NO^+$ species [Eq. 2]. In the presence of H_2O, the formation of HONO is facile:

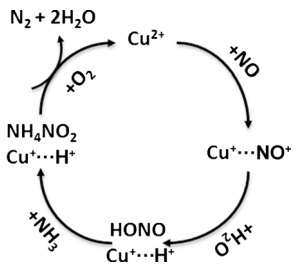

Figure 4. Proposed mechanism for the selective catalytic reduction of NO with NH_3 over Cu-SSZ-13.

$$Cu^+ \cdots NO^+ + H_2O \rightleftharpoons Cu^+ + H^+ + HONO \quad (3)$$

The HONO can, in turn, react with NH_3 to form ammonium nitrite:

$$HONO + NH_3 \rightleftharpoons NH_4NO_2 \quad (4)$$

The ammonium nitrite can subsequently thermally decompose to produce N_2 and H_2O:

$$NH_4NO_2 \rightleftharpoons N_2 + 2\,H_2O \quad (5)$$

The catalytic cycle is completed by the reoxidation of Cu^+ into Cu^{2+} by oxygen, which is present in the reactant gas stream in great excess. Some of the steps in the proposed mechanism cannot be regarded as elementary (such as the reoxidation of Cu^{2+} into Cu^+) and full understanding of the catalytic cycle will require further detailed studies. Invoking this reaction path for the selective formation of N_2 in the SCR of NO with NH_3 also demonstrates a very interesting mechanistic connection between enzymes and heterogeneously catalyzed reactions. In particular, precise control of the coordination environment around the catalytically active metal centers in enzymes and in the CHA-zeolite-based catalysts studied in this work has enabled the identification of a key reaction intermediate for both systems with a very similar structure.

Received: April 24, 2013
Revised: June 17, 2013
Published online: August 12, 2013

Keywords: IR spectroscopy · NMR spectroscopy · reaction mechanisms · reduction · zeolites

[1] B. Kartal, W. J. Maalcke, N. M. de Almeida, I. Cirpus, J. Gloerich, W. Geerts, H. J. M. O. den Camp, H. R. Harhangi, E. M. Janssen-Megens, K. J. Francoijs, H. G. Stunnenberg, J. T. Keltjens, M. S. M. Jetten, M. Strous, *Nature* **2011**, *479*, 127–130.
[2] P. A. Williams, V. Fulop, E. F. Garman, N. F. W. Saunders, S. J. Ferguson, J. Hajdu, *Nature* **1997**, *389*, 406–412.
[3] I. M. Wasser, S. de Vries, P. Moenne-Loccoz, I. Schroder, K. D. Karlin, *Chem. Rev.* **2002**, *102*, 1201–1234.
[4] E. I. Tocheva, F. I. Rosell, A. G. Mauk, M. E. P. Murphy, *Science* **2004**, *304*, 867–870.
[5] A. Weichsel, J. F. Anderson, S. A. Roberts, W. R. Montfort, *Nat. Struct. Biol.* **2000**, *7*, 551–556.
[6] A. Karlsson, J. V. Parales, R. E. Parales, D. T. Gibson, H. Eklund, S. Ramaswamy, *Science* **2003**, *299*, 1039–1042.
[7] M. D. Carducci, M. R. Pressprich, P. Coppens, *J. Am. Chem. Soc.* **1997**, *119*, 2669–2678.
[8] S. Brandenberger, O. Krocher, A. Tissler, R. Althoff, *Catal. Rev. Sci. Eng.* **2008**, *50*, 492–531.
[9] J. H. Kwak, D. Tran, S. D. Burton, J. Szanyi, J. H. Lee, C. H. F. Peden, *J. Catal.* **2012**, *287*, 203–209.
[10] D. W. Fickel, E. D'Addio, J. A. Lauterbach, R. F. Lobo, *Appl. Catal. B* **2011**, *102*, 441–448.
[11] J. H. Kwak, R. G. Tonkyn, D. H. Kim, J. Szanyi, C. H. F. Peden, *J. Catal.* **2010**, *275*, 187–190.
[12] U. Deka, A. Juhin, E. A. Eilertsen, H. Emerich, M. A. Green, S. T. Korhonen, B. M. Weckhuysen, A. M. Beale, *J. Phys. Chem. C* **2012**, *116*, 4809–4818.

[13] J. H. Kwak, D. Tran, J. Szanyi, C. H. F. Peden, J. H. Lee, *Catal. Lett.* **2012**, *142*, 295 – 301.
[14] A. Grossale, I. Nova, E. Tronconi, D. Chatterjee, M. Weibel, *J. Catal.* **2008**, *256*, 312 – 332.
[15] H. Zhu, J. H. Kwak, C. H. F. Peden, J. Szanyi, *Catal. Today* **2013**, *205*, 16 – 23.
[16] J. Szanyi, J. H. Kwak, H. Zhu, C. H. F. Peden, *Phys. Chem. Chem. Phys.* **2013**, *15*, 2368 – 2380.
[17] F. Gao, E. D. Walker, E. M. Karp, J. Y. Luo, R. G. Tonkyn, J. H. Kwak, J. Szanyi, C. H. F. Peden, *J. Catal.* **2013**, *300*, 20 – 29.
[18] J. H. Kwak, H. Y. Zhu, C. H. F. Peden, J. Szanyi, *Chem. Commun.* **2012**, *48*, 4758 – 4760.
[19] D. W. Fickel, R. F. Lobo, *J. Phys. Chem. C* **2010**, *114*, 1633 – 1640.
[20] M. Valiev, E. J. Bylaska, N. Govind, K. Kowalski, T. P. Straatsma, H. J. J. Van Dam, D. Wang, J. Nieplocha, E. Apra, T. L. Windus, W. de Jong, *Comput. Phys. Commun.* **2010**, *181*, 1477 – 1489.
[21] A. D. Becke, *J. Chem. Phys.* **1993**, *98*, 5648 – 5651.
[22] A. Schäfer, H. Horn, R. Ahlrichs, *J. Chem. Phys.* **1992**, *97*, 2571 – 2574.
[23] J.-S. McEwen, T. Anggara, W. F. Schneider, V. F. Kispersky, J. T. Miller, W. N. Delgass, F. H. Ribeiro, *Catal. Today* **2012**, *184*, 129 – 144.
[24] M. Bak, J. T. Rasmussen, N. C. Nielsen, *J. Magn. Reson.* **2000**, *147*, 296 – 330.